

Structural Studies of Chiral Receptors Incorporating D-Glucose

Cristina Vicent,^a Jesús Jiménez-Barbero,^{*a} Manuel Martín-Lomas,^a Soledad Penadés,^{*a} Félix H. Cano^b and Concepción Foces-Foces^b

^a Instituto de Química Orgánica, CSIC, Juan de la Cierva 3, 28006-Madrid, Spain

^b Instituto Rocasolano, CSIC, Serrano 119, 28006-Madrid, Spain

The conformation in solution of the symmetric chiral tetra-*gluco*-24-crown-8 (**1**, R = Bn and **2**, R = Ac), bis-*gluco*-15-crown-5 (**3**, R = Bn and **4**, R = Ac) and bis-*gluco*-21-crown-7 (**5**, R = Bn and **6**, R = Ac) has been established using ¹H NMR spectroscopy. The solid state structure of bis-*gluco*-15-crown-5 (**4**) has also been determined by X-ray diffraction studies and molecular mechanics calculations. All crowns have the same conformation in the 1,2-di-*O*-(3,4,6-tri-*O*-benzyl-β-D-*gluco*-pyranosyl)-ethylene glycol fragment common to all the molecules.

The design of molecular receptors is concerned with the structural arrangement of the binding sites and the stereochemistry of the intermolecular interactions.¹ A careful conformational analysis of the free receptor as well as the complex may lead to a better understanding of the stability and selectivity of the association substrate-receptor. ¹H NMR spectroscopy² and X-ray crystallography together with molecular mechanics³ and, more recently, molecular dynamics⁴ have been used in the study of the relative stability of receptor conformation both in the absence and in the presence of a substrate.

Carbohydrates are complex molecules whose structural features may strongly influence the geometry and the complexing properties of the receptors incorporating them.⁵

We are involved in the synthesis of the new chiral macrocycles with different flexibility and cavity shapes from carbohydrates and in the study of their properties in enantiomeric differentiation and stereoselective catalysis.⁶ We have recently synthesised the symmetrically-substituted chiral tetra-*gluco*-24-crown-8 (**1**), bis-*gluco*-15-crown-5 (**3**) and bis-*gluco*-21-crown-7 (**5**) following a strategy based on the glycosylation of diols with carbohydrate orthoester derivatives.⁷ These receptors have been used as catalysts in the asymmetric Michael addition of methyl α-phenylacetate to methyl acrylate.⁷

The conformational tendency of these crown ethers is dictated by the conformational preferences of the glucopyranose ring and by the *exo*-anomeric effect acting on the glycosidic oxygens which are included in the crown ether cavity. The knowledge of the stereochemistry of complex formation and the understanding of chiral discrimination in these complex systems requires a previous study of the conformation of the receptors. We now report on the solid state structure and solution conformation of bis-*gluco*-15-crown-5 (**4**) and the solution conformation of bis-*gluco*-15-crown-5 (**3**), bis-*gluco*-21-crown-7 (**5** and **6**), and tetra-*gluco*-24-crown-8 (**1** and **2**). The complexing properties of all these receptors with chiral and non-chiral ammonium salts have also been investigated.

Experimental

The synthesis of compounds (**1**–**7**) has been published elsewhere.⁷

¹H NMR spectra were recorded at 300 MHz using a Varian XL-300 spectrometer. the ¹H shift-correlated (COSY) 2D NMR spectra were acquired using the pulse sequence 90°-*t*₁-45°-*t*₂. ¹³C NMR spectra were recorded at 50 MHz on a Bruker AM-200 spectrometer. The XHCORRD pulse sequence pro-

vided by Bruker was used for the heteronuclear correlation experiments.

X-Ray Crystallography.—Crystals of **4** (m.p. 150–151 °C) suitable for X-ray investigation were grown by slow diffusion of hexane in a solution of **4** in ethyl acetate. Table 1 shows the characteristics of the X-ray analysis and Table 2 gives the final fractional coordinates according to the numbering scheme given in Fig. 1.⁸ Tables of thermal parameters and hydrogen atom coordinates have been deposited at the Cambridge Crystallographic Data Centre (CCDC).*

Molecular Mechanics Calculations.—The MM2 (85) programme was used.^{20b} The complete steric energy was calculated using a value of ε 10, which has been stated as a suitable bulk relative permittivity for chloroform solutions.^{20c} The acetyl groups were not included in the minimisation process.

Solid-Liquid Extractions.—Solutions of the hosts in CDCl₃ (0.01–0.2 mol dm⁻³) were mixed with solid benzylammonium thiocyanate (15 mg) for 1 min, filtered several times to ensure that no solid was present in the solution and the ¹H NMR spectra recorded.

Liquid-Liquid Extractions.—Solutions (0.8 cm³) of the host in CDCl₃ (0.02–0.03 mol dm⁻³) were mixed at room temperature with a D₂O solution (0.25 cm³) of α-phenylethylammonium bromide (1 mol dm⁻³) and lithium hexafluorophosphate (1 mol dm⁻³) for 15 min. In the case of **1** and **2**, lithium hexafluorophosphate (2 mol dm⁻³) was added and the extraction was carried out at -10 °C. The phases were separated and the chloroform solution was carefully removed with a syringe, dried and the spectra recorded.

Results and Discussion

The structural analysis of the chiral crown ethers **1**–**6** involved the study of the conformation of the pyranoid ring and the interglycosidic ethylene glycol linkages, which has been carried out following the methodology used in the conformational analysis of oligosaccharides,⁹ and the study of the conformation of the polyethylene glycol chain.

NMR Study of the Crown Ethers.—The ¹H NMR parameters for **1**–**6** and their acyclic precursor **7** in CDCl₃ are given in Table

* For details of the CCDC deposition scheme, see 'Instructions for Authors, (1991), *J. Chem. Soc., Perkin Trans. 2*, in the January issue.

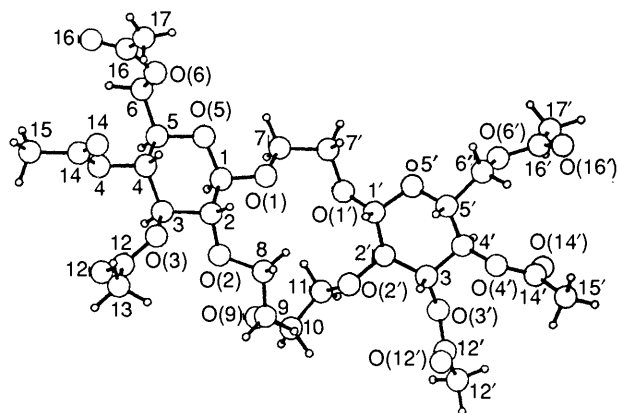
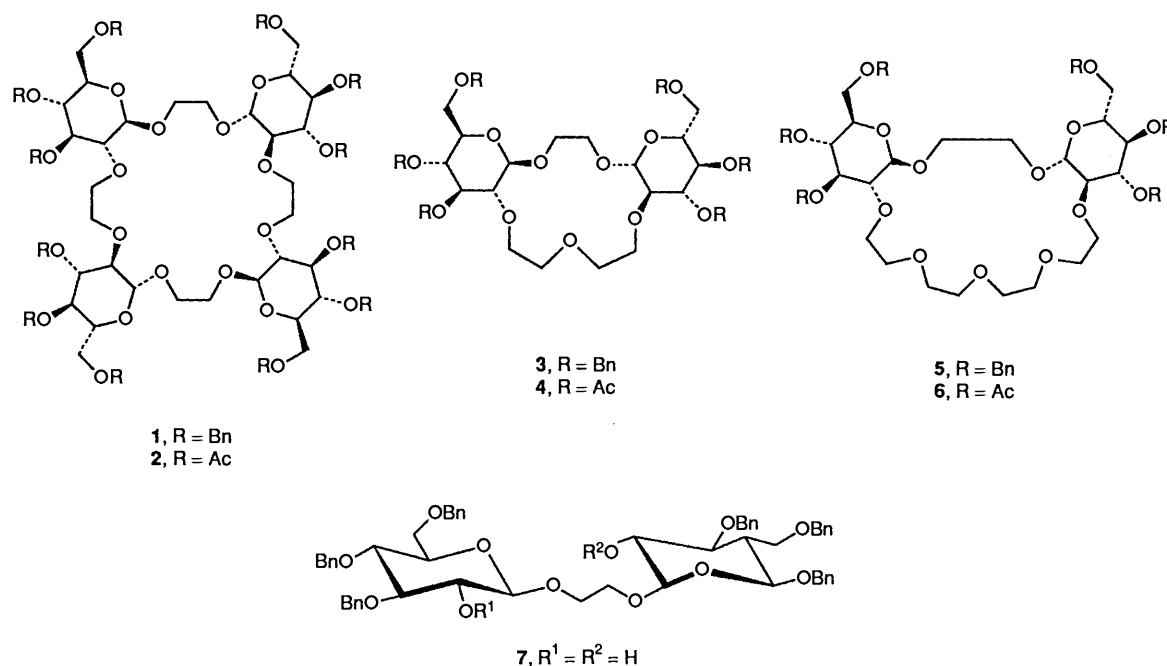


Fig. 1 A view of the bis-*gluco*-15-crown-5 (4) as found in the crystal structure, showing the numbering system

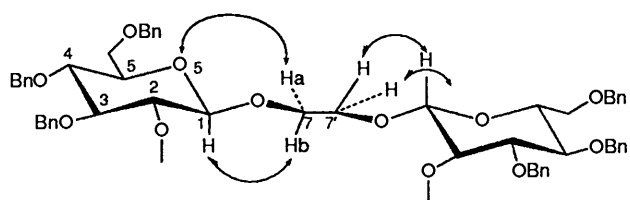


Fig. 2 The proposed conformation for the common part of macrocycles 1-6

3. The proton signals were assigned by conventional COSY spectra and by comparison with those of 7. The ¹³C NMR chemical shifts obtained through 2D carbon-proton correlation experiments are shown in Table 4. All compounds exhibited similar spectral characteristics, especially in the 1,2-di-*O*-(3,4,6-tri-*O*-benzyl-β-D-glucopyranosyl)-ethylene glycol fragment common to all molecules (Fig. 2), and the spectra indicated the symmetry of these molecules in solution (three C₂ axes for 1 and 2 and one C₂ axis for 3-7, the faces of all the chiral crown ethers being homotopic).

The conformation of the pyranoid rings of 1-7 can be described as a ⁴C₁ chair according to the vicinal proton-proton coupling constant values. The population of rotamers of the

hydroxymethyl group, as expected for glucopyranoses,¹⁰ is *ca.* 60:40 for the *gauche-gauche* and *gauche-trans* rotamers as indicated by the *J*_{5-H,6-H} values (Table 3). The size of the crown ether ring does not affect the conformation of the sugar moiety. The conformation around the glycosidic bond can be described by the torsion angles Φ [O(5)-C(1)-O(1)-C(7)] influenced by a number of steric and stereoelectronic effects, mainly the *exo-anomeric* effect,¹⁰ and the more flexible Ψ [C(1)-O(1)-C(7)-C(7')] angle. Conformational studies on alkyl β-D-glucopyranosides gave values for Φ of *ca.* -60° (*g*⁻) and Ψ *ca.* -130° and -180°.¹¹ The known β-configuration of the glycosidic bonds in compounds 1-7 and the different chemical shift values of the diastereotopic interglycosidic ethylene glycol protons 7a-H, 7b-H (Fig. 2) gave information on the conformation of this part of the molecule. The deshielding observed for 7a-H (4.0-4.11) in all crown ethers as compared with 7b-H (3.70-3.85, Table 3) can be explained by an H/O interaction between the lower field proton of the ethylene glycol moiety and the oxygen atom of the glucopyranosidic ring. This interaction does not affect the higher field proton situated further away from the ring oxygen.

This relative orientation of the ethylene glycol moiety with respect to the pyranoid ring (Fig. 2) is stabilized by a double *exo-anomeric* effect which places both glycosidic angles in a *g*⁻ orientation and the O(1)-C(7)-C(7')-O(1') angle in a *g*⁺ orientation.

Taking into account the already fixed *g*⁻ orientation of the O(1)-C(1)-C(2)-O(2) angle, the preferred conformation of this diglycosyl ethylene glycol moiety may be described by a sequence *g*⁻ *g*⁺ *g*⁻. The experimental data (Table 3) indicate that all crown ethers studied 1-6 and the acyclic precursor 7 may have a similar sequence.

The introduction of the polyethylene glycol chain at the O-2 positions of the glucopyranoid rings causes a shielding of the signal assigned to the 2-H protons in all macrocycles, this shielding being more pronounced (Δδ ≈ 0.39) in the spectrum of the bis-*gluco*-15-crown-5 (3). These results indicate a closer proximity of these protons to the methylene groups of the polyethylene glycol chain in these smaller macrocycles than in the tetra-*gluco*-24-crown-8 (1 and 2) and bis-*gluco*-21-crown-7 (5 and 6).

The conformational equilibrium of the polyethylene glycol chain has been studied considering the expected tendency of the

Table 1 Crystal analysis parameters at room temperature

Crystal data	
Formula	C ₃₀ H ₄₄ O ₁₉
Crystal habit	Transparent plate
Crystal size/mm	0.50 × 0.40 × 0.07
Symmetry	Monoclinic, <i>P</i> 2 ₁
Unit cell determination	Least-squares fit from 55 reflections with $\theta < 45^\circ$
Unit cell dimensions	22.5866(20), 14.7060(8), 5.4782(1) Å 90, 93.395(5), 90°
Packing:	
<i>V</i> /Å ³	1816.4(2)
<i>Z</i>	2
<i>D_c</i> /g cm ⁻³	1.296
<i>M</i>	708.67
<i>F</i> (000)	752
μ /cm ⁻³	8.94
Experimental data	
Technique	Four-circle diffractometer Bisecting geometry Graphite-oriented monochromator: Cu <i>K</i> α , $\omega/2\theta$ Detector apertures 1.0 × 1.0°
Total measurements	Up to 65° in θ
Speed	1 min per reflection
Number of reflections:	
Independent	3232
Observed	2455 [$3\sigma(I)$ criterion]
Standard reflections:	2 reflections every 90 min No variation
Solution and refinement	
Solution	Direct methods
Refinement	L.S. on <i>F</i> _{obs} ; 3 blocks
Parameters:	
Number of variables	617
Degrees of freedom	1838
Ratio of freedom	4.0
Hydrogen atoms	All from difference synthesis
Goodness of fit	1.3
Final shift/error	0.16
Weighting scheme	Empirical as to give no trends in $\langle \omega \Delta^2 F \rangle$ vs. $\langle F_{\text{obs}} \rangle$ or $\langle \sin \theta / \lambda \rangle$
Maximum thermal value	<i>U</i> ₁₁ [O(16')] = 0.267(8) Å ²
Final ΔF peaks	0.50 e Å ⁻³
Final <i>R</i> and <i>R_w</i> values	0.041, 0.048
Computer and programs	VAX 11/750 XRAY76 System ²¹ MULTAN80 ²²
Scattering factors	International Tables for X-Ray Crystallography ²³

Table 2 Final atomic coordinates for compound 4

Atom	<i>x/a</i>	<i>y/b</i>	<i>z/c</i>
O(1)	0.1666(1)	0.5000	0.1845(5)
O(2)	0.2207(1)	0.6721(2)	0.0413(6)
O(3)	0.1307(1)	0.7889(2)	-0.1701(5)
O(4)	0.0383(1)	0.8120(2)	0.1732(5)
O(5)	0.0836(1)	0.5782(2)	0.2602(5)
O(6)	-0.0408(1)	0.6187(2)	0.1586(6)
O(9)	0.3411(2)	0.6510(3)	0.1970(10)
O(12)	0.1600(2)	0.9145(2)	0.0324(6)
O(14)	-0.0245(2)	0.8168(3)	-0.1595(8)
O(16)	-0.1163(2)	0.7049(4)	0.2559(8)
C(1)	0.1455(2)	0.5856(3)	0.2395(8)
C(2)	0.1603(2)	0.6499(3)	0.0320(7)
C(3)	0.1272(2)	0.7397(3)	0.0569(7)
C(4)	0.0627(2)	0.7260(3)	0.1062(7)
C(5)	0.0567(2)	0.6631(3)	0.3193(7)
C(6)	-0.0066(2)	0.6458(3)	0.3783(8)
C(7)	0.1618(2)	0.4348(3)	0.3785(9)
C(8)	0.2588(2)	0.6100(4)	-0.0783(11)
C(9)	0.3198(2)	0.6470(4)	-0.0506(13)
C(10)	0.3861(3)	0.5885(5)	0.2731(16)
C(11)	0.3666(3)	0.4925(5)	0.3302(14)
C(12)	0.1460(2)	0.8775(3)	-0.1558(8)
C(13)	0.1431(3)	0.9206(4)	-0.4016(9)
C(14)	-0.0069(2)	0.8484(3)	0.0330(9)
C(15)	-0.0292(2)	0.9314(4)	0.1494(11)
C(16)	-0.0947(2)	0.6542(3)	0.1151(9)
C(17)	-0.1224(2)	0.6264(4)	-0.1226(10)
O(1')	0.2522(1)	0.3574(2)	0.3038(6)
O(2')	0.3536(1)	0.4459(2)	0.1042(7)
O(3')	0.4404(1)	0.3045(3)	0.0313(7)
O(4')	0.3878(1)	0.1731(3)	-0.3198(5)
O(5')	0.2688(1)	0.2346(2)	0.0656(6)
O(6')	0.2876(2)	0.0490(3)	0.0182(7)
O(12')	0.4723(3)	0.3668(7)	-0.3054(16)
O(14')	0.4448(4)	0.0749(6)	-0.1084(9)
O(16')	0.2921(4)	-0.0736(4)	-0.2128(10)
C(1')	0.2787(2)	0.3296(3)	0.0919(9)
C(2')	0.3442(2)	0.3507(3)	0.1285(9)
C(3')	0.3798(2)	0.3020(3)	-0.0624(9)
C(4')	0.3614(2)	0.2060(3)	-0.1044(8)
C(5')	0.2947(2)	0.1997(4)	-0.1470(10)
C(6')	0.2723(2)	0.1037(4)	-0.1894(11)
C(7')	0.1891(2)	0.3479(3)	0.2966(10)
C(12')	0.4819(3)	0.3385(5)	-0.1050(18)
C(13')	0.5415(3)	0.3321(8)	0.0347(24)
C(14')	0.4288(3)	0.1070(5)	-0.2986(10)
C(15')	0.4522(4)	0.0831(8)	-0.5356(12)
C(16')	0.2965(3)	-0.0405(4)	-0.0149(13)
C(17')	0.3079(4)	-0.0902(6)	0.2135(16)

O-C-C-O ethylene glycol fragments to adopt an all *gauche* conformation. The signal for one of the methylene protons in the fragments O(2)-C(8)-C(9)-O(9) of bis-*gluco*-15-crown-5 (**3**) appears as a double triplet at δ 3.72 ppm with coupling constants $^2J = 10.4$ Hz and $^3J = ^3J' = 4.0$ Hz (from first-order analysis), indicating an important contribution of the *gauche* rotamer for this fragment.^{2a} The maintenance of a $g^+g^-g^+g^-g^+$ sequence for the O-C-C-O segments of the pentaethylene glycol chain, the O(2)-C(2)-C(1)-O(1) fragments being already fixed as g^- , should force the fragment O(2)-C(8)-C(9)-O(9) to adopt a g^+ conformation and cause a flattening of the cavity.

A similar argument may be invoked to assign the conformation of the bis-*gluco*-21-crown-7 (**5** and **6**). In this case a similar set of coupling constants can be observed for one of the methylene protons of the O-C-C-O segments of the polyethylene glycol chain. Due to the size of macrocycles **5** and **6** the two additional ethylene glycol segments, as compared with **3** and **4**, should have a greater mobility in solution, fast on the NMR time scale, leading to a rapid conversion of all-*gauche* rotamers.

The tetra-*gluco*-24-crown-8 **1** and **2** can adopt a sequential g^-g^+ conformation for all O-C-C-O torsion angles. The rigidity imposed by the equatorial arrangement of O(1) and O(2) causes a rather flattened structure.

Solid-state Structure of Ethylene (3,3',4,4',6,6'-Hexa-O-acetyl-2,2'-O-oxydiethylene)-di-β-D-glucopyranoside (4).—The solid state structure of **4** was carried out by X-ray diffraction. A PLUTO⁸ view of the molecule is given in Fig. 1. Table 5 gives the main geometrical features of the molecule. The chirality and β -configuration of the solved structure was assessed by means of the configurational angles.¹² For any given sequence around a ring, the configurational angles for a substituent is defined by substrating the corresponding intracyclic torsion angles from that corresponding to the substituent, e.g. in this case, $[C(3)-C(4)-C(5)-C(6)] - [C(3)-C(4)-C(5)-O(5)]$ defines $\rho[C(5)-O(5)]$ after the C(3)-C(4)-C(5)-C(6) sense. It reflects the effect of flattening the ring so as to have the substituent above/below that plane, so giving values of $\pm 120^\circ$. $\rho[C(5)-O(5)] = -\rho[C(5)-C(6)] = -\{\tau[C(3)-C(4)-C(5)-C(6)] -$

Table 3 ^1H NMR data for solutions of 1–7 in CDCl_3 at 30°C

Parameter	Compound						
	1	3	5	2	4	6	7
Chemical shift ^a							
1-H	4.40	4.34	4.38	4.49	4.49	4.47	
2-H	3.38	3.19	3.28	3.37	3.30	3.34	ca. 3.58
3-H	3.52–3.58	3.57	3.60	5.06	5.14	5.11	ca. 3.58
4-H	3.52–3.58	3.50	3.56	4.92	4.98	5.00	ca. 3.58
5-H	3.45	3.37	3.41	3.61	3.55–3.60	3.56–3.60	3.55
6a-H	3.73	3.52–3.60	3.60–3.70	4.21	<i>d</i>	4.27	3.73
6b-H	3.66	3.52–3.60	3.60–3.70	4.03	<i>d</i>	4.11	3.67
ET-1 ^b	4.11/3.75	4.05/3.70	4.04/3.85	4.03/3.82	3.99/3.75	4.05/3.85	4.03/3.82
ET-2 ^c	3.92/3.88	4.06/3.72	4.11/3.75	3.74/3.70	3.60–3.70	3.50–3.70	—
ET-3 ^c	—	3.60/3.65	3.60/3.70	—	3.60–3.70	3.50–3.70	—
<i>J</i> /Hz							
<i>J</i> _{1,2}	7.7	7.8	7.8	7.8	7.8	7.8	7.4
<i>J</i> _{2,3}	9.2	8.4	8.5	9.4	9.3	8.7	<i>d</i>
<i>J</i> _{3,4}	<i>d</i>	9.1	9.0	9.6	9.4	9.5	<i>d</i>
<i>J</i> _{4,5}	<i>d</i>	9.1	9.0	9.8	9.6	9.8	9.2
<i>J</i> _{5,6a}	1.9	2.1	1.9	2.3	<i>d</i>	2.3	2.4
<i>J</i> _{5,6b}	4.5	4.2	4.5	4.7	<i>d</i>	4.7	4.4
<i>J</i> _{6a,6b}	–10.6	–10.4	<i>d</i>	–12.4	<i>d</i>	–12.4	–10.0

^a δ ppm from TMS. ^b Interglycosidic ethylene glycol protons (AB system). ^c Non-interglycosidic ethylene glycol protons. ^d Not determined.

Table 4 ^{13}C NMR chemical shifts for compounds 1–6 in CDCl_3 at 30°C

Chemical shift (δ)	Compound					
	1	3	5	2	4	6
C-1	104.6	101.9	103.6	103.9	102.8	106.8
C-2	82.8	82.5	82.9	79.9	80.5	79.7
C-3	84.5	83.8	84.5	79.2	74.3	73.8
C-4	77.5	76.8	77.6	76.6	73.7	72.0
C-5	74.6	74.6	74.7	76.6	71.6	71.5
C-6	68.9	67.8	68.8	62.0	62.0	62.0
ET-1	71.2	72.2	72.0	71.0	70.6	71.0
ET-2	70.8	69.5	71.0	68.2	68.9	70.2
ET-3	—	69.4	70.6	—	68.7	70.2
ET-4	—	—	70.1	—	—	69.2
ET-5	—	—	68.8	—	—	68.4
PhCH ₂ O	75.3	73.9	75.5	—	—	—
	74.9	73.9	75.0	—	—	—
	73.4	72.5	73.4	—	—	—

$\tau[\text{C}(3)\text{--C}(4)\text{--C}(5)\text{--O}(5)] = -[(179.4) - (-62.3)] \approx +120^\circ$, and analogously $\rho[\text{C}(5')\text{--O}(5')] \approx +120^\circ$. In the same way $\rho[\text{C}(1)\text{--O}(1)] = \tau[\text{O}(1)\text{--C}(1)\text{--O}(5)\text{--C}(5)] - \tau[\text{C}(2)\text{--C}(1)\text{--O}(5)\text{--C}(5)] = 178.1 - (-64.2) \approx -120^\circ$, and so is $\rho[\text{C}(1')\text{--O}(1')]$. Both pyranoid rings are in the expected $^4\text{C}_1$ chair conformation with some flattening around C(2)–C(3) and correspondingly C(2')–C(3'). The hydroxymethyl chain shows a *gauche-gauche* orientation. Almost all the acetyl groups are in the fully extended conformation with the oxygen atoms alternating inside for each chain (Fig. 1). The structure of the glycopyranose moieties follows the pattern for β -pyranoses,¹³ with the C–O inner bonds shorter than the outer ones. The values of both Φ angles are very similar (-66° and -64°) confirming that a double *exo*-anomeric effect operates. However, Ψ angles are rather different (-117° and -131°) but nevertheless in agreement with values previously found in β -glycosides.¹⁴ The constitution of the 15-crown-5 has bond lengths and angles according to the literature,¹⁵ with ranges of C–O [1.385(4)–1.441(5) Å], C–C [1.481(7)–1.530(6) Å], O–C–C [107.2(3)–117.0(5) $^\circ$] and C–O–C [113.7(3)–117.0(5) $^\circ$]. The conformation of this cycle can be described as $e^+ g^+ a^+, g^+ g^- a^+, a^- g^+ e^-, a^+ g^- e^+, a^+ g^+ g^-$, starting at C(10)–O(9)–C(9)–C(8) and moving clockwise (Tables 5 and 6), where $e^+/-$ stands for

$120 \pm 30^\circ$, $g^+/-$ for $60 \pm 30^\circ$ and $a^+/-$ for $180 \pm 30^\circ$ (here simply removing the π modulus of the torsion angles in order to take the 2π modulus). A pseudobinary axis is located between C(7)–C(7') and O(9) and leaves two oxygen atoms on one side of the cycle and three on the other side. This conformation is similar to that adopted by 15-crown-5 ethers when the two faces of the cycle are implicated in the complexation^{16–18} but with departures of five of the C–O–C angles, those underlined above, from the *a* situation.

Fig. 3 shows the situation of the lone pairs on the oxygen atoms¹⁹ with respect to the bulky van der Waals atomic model (see text in the Figure caption concerning the long-pair setting). The less-hindered oxygen atoms O(1) and O(2') appear first with a lone-pair electron each. On moving up in sections the rest of the oxygen atoms are disclosed.

Molecular Mechanics Calculations.—Molecular mechanics calculations have provided a satisfactory description of the conformations of a number of molecules.^{20a} The application of the MM2 program using as initial coordinates those obtained in the X-ray analysis of **5** provided a structure quite similar to that found in the solid state, with an average deviation of 9° for the

Table 5 Selected bond lengths/Å, bond angles/° and torsion angles/° for compound 4

C(1)–O(5)	1.414(5)	O(5)–C(5)	1.434(5)
O(5')–C(1')	1.422(6)	O(5')–C(5')	1.429(6)
O(1)–C(1)	1.385(4)	O(1)–C(7)	1.441(5)
O(1')–C(1')	1.397(6)	O(1')–C(7')	1.432(5)
O(2)–C(2)	1.401(5)	O(2)–C(8)	1.440(6)
O(9)–C(9)	1.414(9)	O(9)–C(10)	1.414(8)
C(1)–C(2)	1.530(6)	C(7)–C(7')	1.499(7)
C(8)–C(9)	1.481(7)	C(10)–C(11)	1.517(10)
C(11)–O(2')	1.430(8)	O(2')–C(2')	1.424(6)
C(1')–C(2')	1.514(6)		
C(1)–O(5)–C(5)	112.7(3)	O(1)–C(1)–O(5)	107.6(3)
C(1)–O(1)–C(7)	113.7(3)	C(1')–O(1')–C(7')	115.0(4)
O(2)–O(2)–C(8)	116.3(3)	C(9)–O(9)–C(10)	117.0(5)
C(11)–O(2')–C(2')	114.5(4)	C(1')–O(5')–C(5')	111.5(4)
O(1')–C(1')–O(5')	107.4(4)	O(1)–C(1)–C(2)	107.9(3)
O(2)–C(2)–C(1)	111.8(3)	O(1)–C(7)–C(7')	107.2(4)
C(2)–C(8)–C(9)	107.4(5)	O(9)–C(9)–C(8)	112.0(5)
O(9)–C(10)–C(11)	117.0(5)	C(10)–C(11)–O(2')	108.4(6)
O(1')–C(1')–C(2')	107.0(4)	O(2')–C(2')–C(1')	109.8(4)
C(7)–C(7')–O(1')	109.6(4)		
C(1)–O(5)–C(5)–C(6)	–170.7(3)	C(1')–O(5')–C(5')–C(6')	–169.1(4)
O(1)–C(1)–C(2)–C(3)	168.5(3)	O(1')–C(1')–C(2')–C(3')	165.7(4)
O(2)–C(2)–C(3)–C(4)	–167.3(3)	O(2')–C(2')–C(3')–C(4')	–164.1(4)
O(3)–C(3)–C(4)–C(5)	171.3(3)	O(3')–C(3')–C(4')–C(5')	167.0(4)
O(4)–C(4)–C(5)–O(5)	–177.1(3)	O(4')–C(4')–C(5')–O(5')	–178.6(3)
C(1)–O(5)–C(5)–C(4)	65.7(4)	C(1')–O(5')–C(5')–C(4')	67.7(5)
C(5)–O(5)–C(1)–C(2)	–62.4(4)	C(5')–O(5')–C(1')–C(2')	–62.9(5)
O(5)–C(1)–C(2)–C(3)	50.5(4)	O(5')–C(1')–C(2')–C(3')	48.8(5)
C(1)–C(2)–C(3)–C(4)	–46.4(4)	C(1')–C(2')–C(3')–C(4')	–43.5(6)
C(2)–C(3)–C(4)–C(5)	52.1(4)	C(2')–C(3')–C(4')–C(5')	49.3(5)
C(3)–C(4)–C(5)–O(5)	–59.1(4)	C(3')–C(4')–C(5')–O(5')	–59.8(5)
C(7)–O(1)–C(1)–O(5)	–66.3(4)	C(7')–O(1')–C(1')–O(5')	–64.2(5)
C(10)–O(9)–C(9)–C(8)	109.1(6)	O(9)–C(9)–C(8)–O(2)	63.3(6)
C(9)–C(8)–O(2)–C(2)	178.9(4)	C(8)–O(2)–C(2)–C(1)	86.2(4)
O(2)–C(2)–C(1)–O(1)	–74.2(4)	C(2)–C(1)–O(1)–C(7)	173.3(3)
C(1)–O(1)–C(7)–C(7')	–177.2(3)	O(1)–C(7)–C(7')–O(1')	73.0(4)
C(7)–C(7')–O(1')–C(1')	–131.0(4)	C(7')–O(1')–C(1')–C(2')	176.4(4)
O(1')–C(1')–C(2')–O(2')	–74.8(4)	C(1')–C(2')–O(2')–C(11)	105.0(5)
C(2')–O(2')–C(11)–C(10)	170.1(5)	O(2')–C(11)–C(10)–O(9)	76.8(7)
C(11)–C(10)–O(9)–C(9)	–80.4(8)		

Table 6 Torsion angles/° for compound 4 calculated by the MM2 program

Torsion angles/°	MM2(°)	Torsion angles/°	MM2(°)
C(7)–O(1)–C(1)–O(5)	–71	C(7')–O(1')–C(1')–O(5')	–59
C(10)–O(9)–C(9)–C(8)	149	O(9)–C(9)–C(8)–O(2)	53
C(9)–C(8)–O(2)–C(2)	–166	C(8)–O(2)–C(2)–C(1)	92
O(2)–C(2)–C(1)–O(1)	–72	C(2)–C(1)–O(1)–C(7)	171
C(1)–O(1)–C(7)–C(7')	–176	O(1)–C(7)–C(7')–O(1')	74
C(7)–C(7')–O(1')–C(1')	–141	C(7')–O(1')–C(1')–C(2')	–178
O(1')–C(1')–C(2')–O(2')	–66	C(1')–C(2')–O(2')–C(11)	105
C(2')–O(2')–C(11)–C(10)	–174	O(2')–C(11)–C(10)–O(9)	65
C(11)–C(10)–O(9)–C(9)	149		

Table 7 Distances among the oxygen atoms involved in the cavity of 4 according to MM2 calculations

	O(1)	O(2)	O(1')	O(2')	O(9)
O(1)	—	2.95	2.91	4.60	4.04
O(2)	2.95	—	4.83	4.78	2.72
O(1')	2.91	4.83	—	2.88	4.09
O(2')	4.60	4.78	2.88	—	2.87
O(9)	4.04	2.72	4.09	2.87	—

macrocyclic ring torsion angles. Although the program is not capable of providing a global minimum, it can be stated that the solid-state structure is at least a local minimum. The values of

the O–C–O angles are very similar to the crystallographic data (Table 6) but there are now seven C–O–C angles in a *trans* or nearly *trans* orientation while the other three are in between *gauche* and *trans* relationships. Table 7 shows the distances among the oxygen atoms involved in the cavity. These distances vary between 2.72 and 2.95 Å for vicinal oxygens, while for non-contiguous oxygens the range is between 4.04 and 4.38 Å. These two distances correspond to the minimum and maximum diameter of the cavity formed by the oxygen atoms.

The conformation found in the solid state and that calculated by MM2 (Fig. 4) are similar to those proposed in solution. This conformation leaves two oxygen atoms on each side of the cycle and the fifth one [O(9) passing through the C(2) axis] either on one side or in between.

It would be expected that this conformation was responsible for complexation on both sides, through O(1) and O(2') and then either through two or three of O(1'), O(2) and O(9). In terms of lone pairs (Fig. 3) the interaction can be performed, in a hindered way, across the cycle through O(1a) and O(2'b) on one side, and on the other side, across the cycle through either two of O(1'b), O(9a) or O(2a).

Complex Formation with Organic Ammonium Salts.—Evidence for host–guest complex formation of 1–5 with benzylammonium thiocyanate was obtained by ¹H NMR spectroscopy. Solutions of hosts 1–5 in CDCl₃ (0.01–0.02 mol dm^{–3}) were shaken at room temperature with an excess of solid

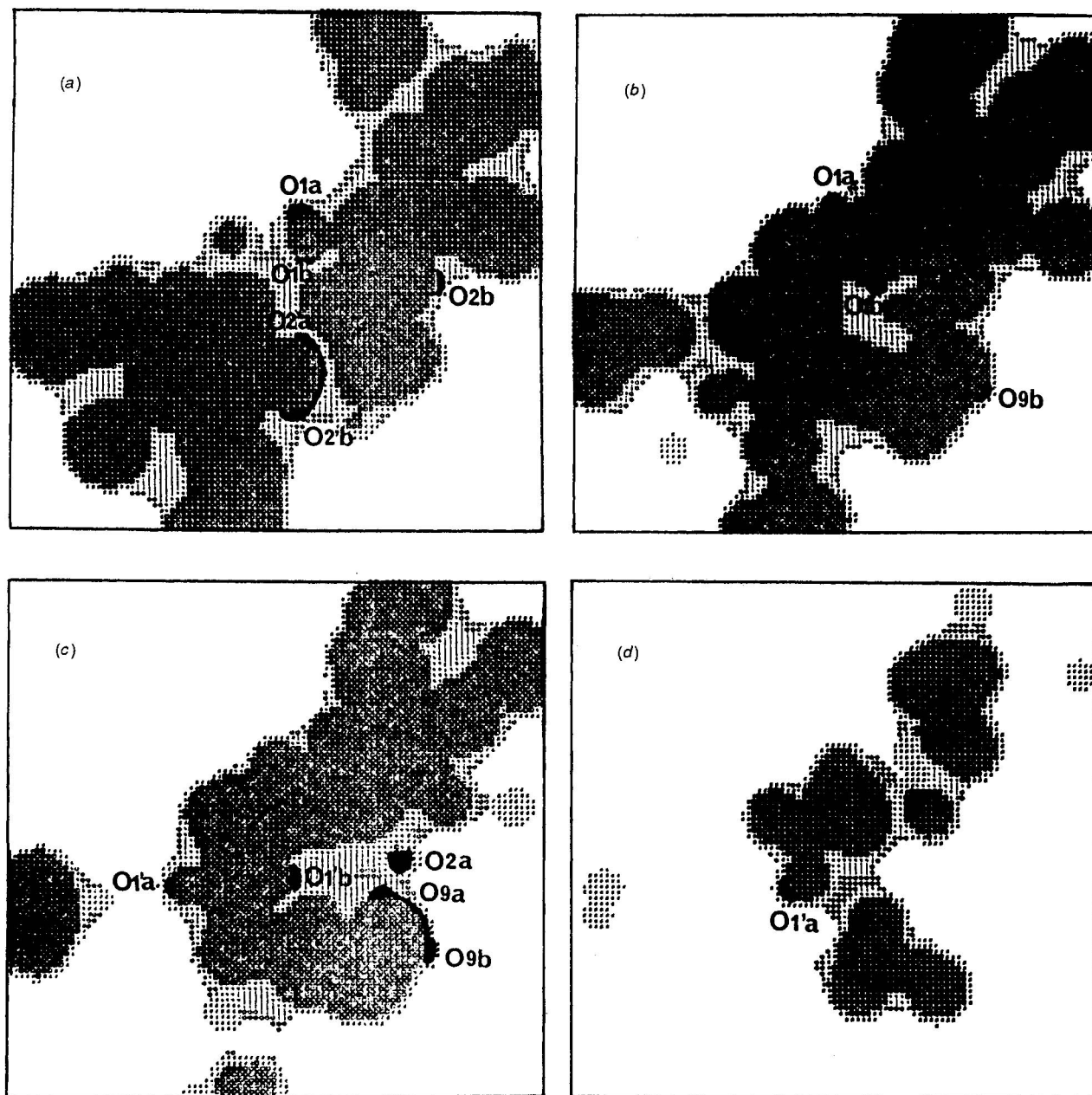


Fig. 3 Crystallographic Z sections, through the van der Waals bulk molecular model, with clefts smoothed with a rolling ball of radius 1 Å. Oxygen lone pairs (dark zone) have been simulated as spheres of radius 0.7 Å and are tetrahedrally positioned around the corresponding oxygen atoms, in order to show their surface on the oxygen van der Waals envelope. The fractional coordinates range is, down the page, $0.33 \leq x \leq 0.68$ and, across the page, $0.23 \leq y \leq 0.79$, for: (a) $z = 0.48$; (b) $z = 0.59$; (c) $z = 0.65$ and (d) $z = 0.78$.

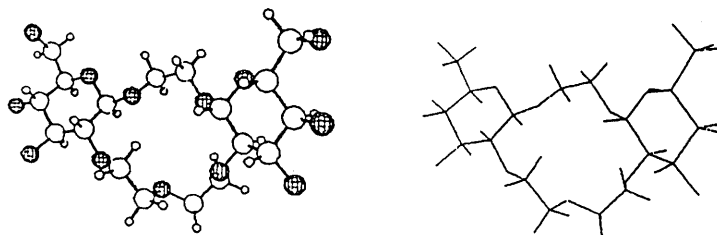


Fig. 4 A view of the minimum obtained by MM2 calculations for macrocycle 4

benzyl ammonium salt and its NMR spectrum was recorded. Integration of the signals of the benzylic protons of the guest molecule *versus* the anomeric protons of the host indicated an extracted 1:1 host:guest molar ratio for the bis-*gluco*-15-crown-5 (3) and bis-*gluco*-21-crown-7 (5) and 1:2 for the tetra-*gluco*-24-crown-8 (2). Molar ratios higher than 1:1 have previously been described for 24-crown-8 derivatives.²⁴

The ¹H NMR spectra of 2 and 3 did not show drastic changes upon complexation; only 2-H showed a shielding of *ca.* 0.03 ppm. In contrast, a dramatic change was observed in the spectrum of the bis-*gluco*-21-crown-7 (5) particularly in the polyether proton region, indicating a conformational change of the polyethylene glycol chain in order to achieve a better interaction with the ammonium salts.²⁵ The most significant

change in the signal assigned to the sugar moiety is the shielding of ca. 0.2 ppm for 2-H.

Chiral recognition experiments were carried out with (*R,S*)- α -phenylethylammonium hexafluorophosphate as the guest following the procedure described in the literature.²⁶ Integration of the signals for the methyl protons of the salt *versus* that of the anomeric protons of the host in the ¹H NMR spectra of the chloroform layer allowed the determination of the molar ratio of the extraction. The bis-*gluco*-15-crown-5 (3) forms diastereoisomeric complexes with the racemic guest. Both the racemic and the enantiomerically pure salts are extracted in a 1:2 host:guest molar ratio. The formation of diastereoisomeric complexes with the racemic salt was evident from the two doublets at 1.46 and 1.45 ppm and two quartets at 4.40 and 4.38 ppm corresponding to the methyl and methine protons of the 3-(*S,S*) and 3-(*RR*) and 3-(*R,S*) complexes, which under the NMR conditions (fast guest exchange) show only two sets of signals for the guest and one set for the host. The changes in the spectrum of the host were minimal and similar to those observed in the complex with benzylammonium salt, the shielding of 2-H being 0.06 ppm. Complexes 1:2 of 15-crown-5 ethers have been described previously²⁴ and their formation can be explained if both faces of the crown ether are involved in the complexation. Taking into account the conformation found for the bis-*gluco*-15-crown-5 (4) in the solid state and in solution (see above), one of the ammonium salts could interact through three hydrogen bonds, two with O(1) and O(2') of a face and the third with an oxygen atom of a water molecule²⁷ or with its counter ion.²⁸ The second molecule could bind to the other face in similar way.

The bis-*gluco*-21-crown-7 (5) forms a complex with the racemic salt in the molar ratio 1:1.2. The formation of diastereoisomeric complexes could not be observed. The chemical shift changes were similar to those described above for the benzylammonium salt, indicating that the interaction takes place with the polyether chain, relatively far away from the chiral centres of the sugar.

The tetra-*gluco*-24-crown-8 (1) showed no complexation ability at room temperature. However, when the extraction was performed with the racemic salt at -10°,²⁹ the diastereoisomeric complexes 1-(*S,S*), 1-(*R,R*) and 1-(*R,S*) were formed in a 1:2 (host:guest) molar ratio. The two doublets at 1.47 and 1.44 ppm and two quartets at 4.26 and 4.12 ppm were assigned tentatively to the methyl and methine protons of the 1-(*S*) and 1-(*R*) complexes, respectively, by comparison with the extraction of the pure enantiomers. The extracted molar ratio for the *S* and *R* enantiomers were 1:1.8 and 1:0.7, respectively. These differences in the molar ratio of extraction could be due to a chiral discrimination process, although other factors, such as the amount of water extracted, have been shown to play an important role in the complexation of alkylammonium salts by large crown ethers.³⁰

The ¹³C NMR spectra of 1-(*R,S*) were also recorded and again the formation of diastereoisomeric complexes was confirmed from the observation of two signals for the methyl and *ipso* carbons of the salt, the intensity of both signals being different. The acetylated derivative tetra-*gluco*-24-crown-8 (2) also formed diastereoisomeric complexes with the racemic salt at -10 °C giving host:guest molar ratios of 1:1.4 for 2-(*R,S*), 1:1.6 for 2-(*S*) and 1:1.8 for 2-(*R*), the changes in the ¹H NMR spectrum being similar to those observed for the benzylammonium complexes.

In conclusion, the structural studies reported here indicate that the conformation in solution of both free and complexed glucose-containing crown ethers 1-6 is very similar. Even the 15-crown-5 (4) adopts in the solid state a conformation similar to that shown by other 15-crown-5 compounds in which the two faces of the macrocycle are implicated in the complexation.¹⁶⁻¹⁸

Acknowledgements

We thank the *Dirección General de Investigación Científica y Técnica* (Grant PB 87-0367 and PB 87-0291) for the financial support. One of us (C. V.) thanks the *Comunidad de Madrid* for a fellowship.

References

- 1 T. H. Crawshaw, D. A. Laidler, J. C. Metcalfe, R. B. Pettman, J. F. Stoddart and J. B. Wolstenholme in *Studies in Organic Chemistry*, vol. 10, eds. B. S. Green, Y. Ashani and D. Chipman, Elsevier, Amsterdam, 1981, p. 49.
- 2 (a) D. Live and S. I. Chan, *J. Am. Chem. Soc.*, 1976, **98**, 3769; (b) P. A. Mosier-Boss and A. I. Popov, *J. Am. Chem. Soc.*, 1985, **107**, 6168; (c) G. W. Buchanan, R. A. Kirby and J. P. Charland, *J. Am. Chem. Soc.*, 1988, **110**, 2477.
- 3 (a) P. A. Kollman, G. Wipff and U. J. Chandra Singh, *J. Am. Chem. Soc.*, 1985, **107**, 2212; (b) B. B. Masek, B. D. Santarsiero and D. S. Dougherty, *J. Am. Chem. Soc.*, 1987, **109**, 4373; (c) J. W. H. M. Uiterwijk, S. Harkema and D. Feil, *J. Chem. Soc., Perkin Trans. 2*, 1987, 721.
- 4 (a) P. D. J. Grootenhuys and P. A. Kollman, *J. Am. Chem. Soc.*, 1989, **111**, 2152; (b) D. Gehin, P. A. Kollman and G. Wipff, *J. Am. Chem. Soc.*, 1989, **111**, 3011.
- 5 J. F. Stoddart, *Chem. Soc. Rev.*, 1979, **8**, 85.
- 6 (a) M. Alonso-López, M. Bernabé, A. Fernández-Mayoralas, J. Jiménez-Barbero, M. Martín-Lomas and S. Penadés, *Carbohydr. Res.*, 1986, **150**, 103; (b) M. Alonso-López, M. Martín-Lomas and S. Penadés, *Carbohydr. Res.*, 1988, **175**, 133; (c) M. Alonso-López, J. Jiménez-Barbero, M. Martín-Lomas and S. Penadés, *Tetrahedron*, 1988, **44**, 1535; (d) M. Alonso-López, M. Martín Lomas and S. Penadés, *Tetrahedron Lett.*, 1986, **27**, 3551; (e) M. Alonso-López, M. Martín-Lomas, S. Penadés, C. Bosso and J. Ulrich, *J. Carbohydr. Chem.*, 1986, **5** (4), 705.
- 7 C. Vicent, M. Martín-Lomas and S. Penadés, *Tetrahedron*, 1989, **45**, 3605.
- 8 W. D. S. Mortherwell and W. Clegg, PLUTO. A Program for Plotting Crystal and Molecular Structures, Cambridge University, UK, 1978.
- 9 K. Bock, *Pure Appl. Chem.*, 1983, **55**, 605.
- 10 J. P. Praly and R. U. Lemieux, *Can. J. Chem.*, 1987, **65**, 213, and references therein.
- 11 R. U. Lemieux and S. Koto, *Tetrahedron*, 1974, **30**, 1933.
- 12 F. H. Cano, C. Foces-Foces, M. Bernabé, J. Jiménez-Barbero, M. Martín-Lomas and S. Penadés, *Tetrahedron*, 1985, **18**, 3875.
- 13 G. A. Jeffrey, J. A. Pople, J. S. Binkley and S. Vishveshwara, *J. Am. Chem. Soc.*, 1978, **100**, 373.
- 14 S. Pérez, *Thèse d'Etat*, Université de Grenoble, 1978.
- 15 R. D. Rogers, L. K. Kurihara and M. M. Benning, *Inorg. Chem.*, 1987, **26**, 4346.
- 16 R. D. Rogers and M. M. Benning, *Acta Crystallogr., Sect. C*, 1988, **44**, 641.
- 17 E. Arte, J. Fenneau-Dupont, J. P. Declercq, G. Germain and M. Van Meerssche, *Acta Crystallogr., Sect. B*, 1979, **35**, 1215.
- 18 R. D. Rogers and L. K. Kurihara, *Inorg. Chim. Acta*, 1987, **129**, 277.
- 19 M. Martínez-Ripoll, F. H. Cano and C. Foces-Foces, *Holes*, 1989, to be published.
- 20 (a) U. Burkert and N. L. Allinger, *Molecular Mechanics*, ACS Monograph 177, Washington, DC, 1982; (b) N. L. Allinger, *QCPE*, 1985, **986**; (c) C. Jaime, E. Osawa, Y. Takenchi and P. Camps, *J. Org. Chem.*, 1983, **48**, 4514.
- 21 J. M. Stewart, P. A. Machin, C. W. Dickinson, H. L. Ammon, H. Heck and H. Flack, *The X-Ray System*. Technical Report TR-446, Computer Science Center, University of Maryland, USA, 1976.
- 22 P. Main, S. J. Fiske, S. E. Hull, L. Lessinger, G. Germain, J. P. Declercq and M. M. Woolfson, MULTAN 80. A System of Computer Programs for the Automatic Solution of Crystal Structures from X-ray Diffraction Data. Universities of York (England) and Louvain (Belgium), 1980.
- 23 *International Tables for X-Ray Crystallography*. Vol. IV, Kynoch Press, Birmingham, UK, 1974. (Present distributor D. Reidel, Dordrecht.)
- 24 M. R. Johnson, N. F. Jones, I. O. Sutherland and R. F. Newton, *J. Chem. Soc., Perkin Trans. 1*, 1985, 1637.
- 25 See, e.g., (a) I. O. Sutherland, *Chem. Soc. Rev.*, 1986, **15**, 63; (b) D. A. Laidler and J. F. Stoddart, *J. Chem. Soc., Chem. Commun.*, 1977, 481.
- 26 E. P. Kyba, J. M. Timko, L. J. Kaplan, F. de Jong, G. W. Gokel and D. J. Cram, *J. Am. Chem. Soc.*, 1978, **100**, 4555.

- 27 (a) J. C. Metcalfe, J. F. Stoddart, G. Jones, T. H. Crawshaw, E. Gavuzzo and D. J. Williams, *J. Chem. Soc., Chem. Commun.*, 1981, 432; (b) D. L. Hughes and J. N. Wingfield, *J. Chem. Soc., Chem. Commun.*, 1977, 804.
- 28 K. M. Doxsee, *J. Org. Chem.*, 1989, **54**, 4712.
- 29 S. C. Peacock, L. A. Domeier, F. C. A. Gaeta, R. C. Helgeson, J. M. Timko and D. J. Cram, *J. Am. Chem. Soc.*, 1978, **100**, 8190.
- 30 F. De Jong, D. N. Reinhoudt and C. J. Smith, *Tetrahedron Lett.*, 1976, 1371.

Paper 0/02942D

Received 2nd July 1990

Accepted 15th February 1991